Permian (Artinskian to Wuchapingian) conodont biostratigraphy in the Tieqiao section, Laibin area, South China

Y.D. Sun[a, b]*, X.T. Liu[c], J.X. Yan[a], B. Li[d], B. Chen[e], D.P.G. Bond[f], M.M. Joachimski[b], P.B. Wignall[g], X.L. Lai[a]

[a] State Key Laboratory of Biogeology and Environmental Geology, China University of Geosciences, Wuhan, 430074, China

[b] GeoZentrum Nordbayern, Universität Erlangen-Nürnberg, Schlossgarten 5, 91054 Erlangen, Germany

[c] Key Laboratory of Marine Geology and Environment, Institute of Oceanology, Chinese Academy of Sciences, Qingdao, 266071, China

[d] Key Laboratory of Marine Mineral Resources, Guangzhou Marine Geological Survey, Ministry of Land and Resources, Guangzhou, 510075, China

[e] State Key Laboratory of Palaeobiology and Stratigraphy, Nanjing Institute of Geology and Palaeontology, 39 East Beijing Road, Nanjing, 210008, R.P. China

[f] School of Environmental Sciences, University of Hull, Hull HU6 7RX, UK

[g] School of Earth and Environment, University of Leeds, Leeds LS2 9JT, UK

*Corresponding authors Email: yadong.sun@cug.edu.cn (Y.D. Sun)

Abstract

Permian strata from the Tieqiao section (Jiangnan Basin, South China) contain several distinctive conodont assemblages. Early Permian (Cisuralian) assemblages are dominated by the genera *Sweetognathus, Pseudosweetognathus* and *Hindeodus* with rare *Neostreptognathodus* and *Gullodus.* Gondolellids are absent until the end of the Kungurian stage—in contrast to many parts of the world where gondolellids and *Neostreptognathodus* are the dominant Kungurian conodonts. A conodont changeover is seen at Tieqiao and coincided with a rise of sea level in the late Kungurian to the early Roadian: the previously dominant sweetognathids were replaced by mesogondolellids. The Middle and Late Permian (Guadalupian and Lopingian Series) witnessed dominance of gondolellids (*Jinogondolella* and *Clarkina*), the common presence of *Hindeodus* and decimation of *Sweetognathus.*

Twenty main and seven subordinate conodont zones are recognised at Tieqiao, spanning the lower Artinskian to the middle Wuchiapingian Stage. The main (first appearance datum) zones are, in ascending order by stage: the *Sweetognathus (Sw.) whitei*, *Sw. toriyamai*, and *Sw. asymmetrica* n. sp. Zones for the Artinskian; the *Neostreptognathodus prayi*, *Sw. guizhouensis*, *Sw. iranicus*, *Sw. adjunctus*, *Sw. subsymmeticus* and *Sw. hanzhongensis* Zones for the Kungurian; the *Jinogondolella (J.) nankingensis* Zone for the Roadian; the *J. aserrata* Zone for the Wordian; the *J. postserrata*, *J. shannoni*, *J. altudaensis*, *J. prexuanhanensis*, *J.*

xuanhanensis, *J. granti* and *Clarkina (C.) hongshuiensis* Zones for the Capitanian and the *C. postbitteri* Zone and *C. transcaucasica* Zone for the base and middle of the Wuchiapingian. The subordinate (interval) zones are the *Pseudosweetognathus (Ps.) costatus*, *Ps. monocornus*, *Hindeodus (H.) gulloides*, *Pseudohindeodus ramovsi*, *Gullodus (G.) sicilianus*, *G. duani* and *H. excavates* Zones.

In addition, three new species, *Gullodus tieqiaoensis* n. sp., *Pseudohindeodus elliptica* n. sp. and *Sweetognathus asymmetrica* n. sp. are described. Age assignments for less common species (e.g., *G. duani, H. catalanoi* and *Pseudosweetognathus monocornus* etc.) are reassessed based on a rich conodont collection.

1. Introduction

Conodonts are important index fossils in the Palaeozoic and Triassic, due to their high speciation rates, geographically widespread distribution and in part high abundance in marine sediments. Conodont biostratigraphy provides the best method for high-resolution, supra-regional correlations of Permian strata, because other key taxa such as ammonoids are often scarce in many locations, whilst foraminifers and brachiopods are generally long ranging and facies controlled and thus less useful for age diagnosis. As a consequence, Permian conodont taxonomy and biostratigraphy have been the topics of extensive study since the 1950s (e.g., Youngquist et al., 1951; Clark and Behnken, 1971; Ritter, 1986; Wardlaw and Grant, 1990; Mei et al., 1994b; Wardlaw, 2000; Nestell et al., 2006; Lambert et al., 2010; Shen et al., 2012). The importance of conodonts in stratigraphy is exemplified by their use at Global Boundary Stratotype Section and Points: as of 2016, conodonts define of the bases of all but three of the 29 stages between the Pragian (Lower Devonian) and Rhaetian (Upper Triassic), 15 of which have been ratified by the International Commission on Stratigraphy.

The diversity of Permian conodonts is generally low in comparison to that observed for other time periods, with typically fewer than five genera and two dozens of species occurring in any given Permian stage. Conodont zones are also relatively long for some intervals. For instance, though substantial investigations have been carried out in West Texas (e.g., Wardlaw, 2000; Nestell et al., 2006; Nestell and Wardlaw, 2010a; Wardlaw and Nestell, 2010), only one standard

conodont zone has been established for the Roadian and Wordian stages (Henderson et al., 2012). This reflects a true low point in the diversity of conodonts during their long evolutionary history. A further complication is that minor changes in Permian conodont morphology require a careful taxonomic examination of different species. New species are rarely reported from regions other than West Texas and South China, perhaps owing to a decrease in research effort and a substantial loss of expertise in recent years.

Establishing a robust biostratigraphic scheme in different areas is essential for supra-regional correlation. Permian conodonts have been most often studied in the Urals of Russia (Early Permian), West Texas (Middle Permian) and South China (Late Permian and the Permo-Triassic boundary) (e.g., Chuvashov et al., 1990; Mei et al., 1994a; Zhang et al., 1995; Wardlaw, 2000; Lambert et al., 2002; Chernykh, 2005; Jiang et al., 2007; Nestell and Wardlaw, 2010b). The Early to Middle Permian of South China has attracted comparatively little research attention and is less systematically studied (Wang et al., 2016).

This study presents a higher-resolution conodont record for the Tieqiao section, Guangxi, South China. New data, spanning the Artinskian (Early Permian) to the middle Wuchiapingian (Late Permian), substantially improve existing records of the section, first described two decades ago in the context of the Capitanian-Wuchiapingian (Guadalupian-Lopingian) transition (Mei et al., 1994c; Henderson et al., 2002; Wang, 2002).

2. Geological setting

The Yangtze region was a large isolated platform situated within the Permian equatorial Tethys (Fig. 1) with extensive carbonate deposits and diverse sedimentary facies. It is an ideal location for conodont studies. The Laibin area is located in the Dian-Qian-Gui Basin towards the southwestern margin of the Yangtze Platform (Wang and Jin, 2000). A series of superb sections are exposed along the banks of Hongshui River (Shen et al., 2007) and these have been comprehensively studied for the Capitanian-Wuchiapingian transition (e.g., Mei et al., 1994c; Wang et al., 2004; Jin et al., 2006; Wignall et al., 2009b; Chen et al., 2011).

The Permian strata of the region consist of thick Early Permian platform carbonates, subordinate Middle Permian slope to basinal carbonates and cherts. Late Permian rocks are geographically more variable, including coal seams, reef build-ups and radiolarian cherts (Sha et al., 1990; Shen et al., 2007; Qiu et al., 2013).

The studied section at Tieqiao (23° 42.733' N, 109° 13.533' E) is exposed on the northern bank of the Hongshui River, southeast of the town of Laibin (Figs. 1, 2). The Permian strata measure 1307 m thick and comprise the Maping, Chihsia, Maokou, Wuchiaping (Heshan) and Talung Formations, spanning the earliest Permian (Asselian) to the Permian-Triassic boundary (Sha et al., 1990). The section is very fossiliferous, with foraminifers, calcareous algae, crinoids, sponges

6

and corals being prolifically abundant (e.g., Wang and Sugiyama, 2000; Bucur et al., 2009; Zhang et al., 2015), whilst bivalves and ammoinods occur less frequently. Well-preserved *Zoophycos* trace fossils are also abundant (Gong et al., 2010).

Sha and colleagues (1990) pioneered the study of the Tieqiao section and subdivided the section into 15 Members and 139 Beds. Our study follows these subdivisions (Figs. 3-5) for consistency and focuses on the stratigraphy and conodont zonation of the Chihsia, Maokou and Wuchiaping Formations (Bed 1 to Bed 134). The Chihsa Fm. generally records deposition in a carbonate ramp setting, whilst the Maokou Fm. comprises slope to basin transition facies. The two formations are 710 m thick in total and range from the Sakmarian (?) to the Capitanian-Wuchiapingian boundary (Figs. 3-5). The Wuchiaping Fm. records a shift in depositional environments from a deep water basin (Beds 120- 122) to a sponge reef (Beds 123-133).

3. Materials and methods

The section was sampled over four field campaigns between 2005 and 2010. During the spring of 2010, the water of the Hongshui River fell to its lowest level of the past ten years due to a severe drought, which allowed us to describe and sample several normally submerged parts of the section (e.g., Bed 17 and Bed 112). A total of 374 rock samples were collected with a sampling resolution of ~1-2 m for most parts of the section. Cherts and grainstones bearing abundant

corals and fusulinid foraminifers were avoided during sampling due to complications in conodont extraction and low conodont yields. Each sample weighed between 2.5 and 8.0 kg.

Three hundred and eleven samples were processed in the micropaleontology laboratory at China University of Geosciences (Wuhan) and 63 samples were processed at the GeoZentrum Nordbayern, Universität Erlangen-Nürnberg. All samples were dissolved using 7-10% diluted acetic acid, wet sieved through 20# and 160# meshes (openings are ~850 and 97 μm, respectively) and air-dried. The insoluble residues were separated by using heavy liquid fractionation (bromoform-acetone solution at Wuhan and sodium polytungstate-water solution at Erlangen, each with density 2.82 g/cm^3). Conodont specimens were handpicked using binocular microscopes. Conodonts from Tieqiao are generally well preserved with colour alternation index ranging from 1.5 to 2.5. A total of 8733 specimens were obtained at Wuhan and about 3000 specimens were recovered at Erlangen. Results from both laboratories were cross checked.

Please note that references to the first appearance datum (FAD) in this study are based on the current sampling effort, and represent the local first occurrence (FO) of a species.

4. Stratigraphy and Conodont Zonation

4.1 Sakmarian (?)

The lowermost part of the studied section (Beds 1 to 16, Chihsia Fm.)

consists mainly of thin-to-medium bedded dark-grey bioclastic micrites, marls and black shales (Fig. 2). Brachiopods, gastropods, crinoids, bryozoans and sponges are the most abundant fossils. The age assignment for this part of the section is controversial. Sha et al. (1990) suggested an Asselian age for the underlying Maping Fm. and reported the occurrence of the fusulinacean foraminifers *Eoparafusulina* sp., *Nankinella* sp., *Pamirina* sp., *Staffella* sp., and *Pseudofusulina* sp. from Bed 1 to Bed 16, implying a possible Sakmarian age for the unit. Mei et al. (1998) inferred this unit to be of "Longlinian" age – a Chinese equivalent of the Artinskian by original definition (Sheng and Jin, 1994; Jin et al., 1997), now re-defined as Sakmarian (Fig. 24.1 in Henderson et al., 2012). Based on consideration of all published fossil materials, Shen et al. (2007) tentatively assign this part of the section to the Artinskian.

Few conodonts were recovered from this part of the section, despite great efforts. Many ramiform elements were recovered from Bed 8, but none is age-diagnostic. These ramiform elements are rather robust and unlikely belong to *Sweetognathus* or *Hindeodus* (e.g., Wardlaw et al., 2015). The precise age of this unit remains unresolved. Here we tentatively assign this unit to the Sakmarian.

4.2 Artinskian

Beds 17 to 26 consist mainly of dark-grey to grey bioclastic pack- and grainstones. The conodont assemblage is dominated by *Sweetognathus whitei* and affinitive species and thus indicates an Artinskian age. *Neostreptognathodus*

and *Hindeodus* are rare whilst gondolellids are absent. The base of the Artinskian stage cannot be precisely defined because the FAD of *Sweetognathus whitei* cannot be ascertained due to the inaccessibility of the submerged lower part of Bed 17 and the absence of diagnostic conodonts from beds below this level. In ascending order, three conodont zones were established for the Artinskian:

1) *Sweetognathus whitei* Zone (?30 - 36.5 m, Bed 17)

The lower limit of this zone is not defined. The upper limit is defined by the FAD of *Sweetognathus* (*Sw.*) *toriyamai*.

Sweetognathus whitei was one of the most cosmopolitan conodont species during the Early Permian (Mei et al., 2002). It is known e.g. from North and South China, Japan, U.S.A., Canada and Colombia. (Rhodes, 1963; Igo, 1981; Orchard, 1984; Ritter, 1986; Ding and Wan, 1990; Ji et al., 2004; Boardman et al., 2009) and is considered a good marker for the base of Artinskian.

2) *Sweetognathus toriyamai* Zone (36.5 – 41 m, Beds 17-18)

Lower limit: FAD of *Sw. toriyamai* in the uppermost Bed 17. Upper limit: FAD of *Sw. asymmetrica* n. sp. The FAD of *Sw. bogoslovskajae* occurs in this zone. *Sw. bogoslovskajae* is known to co-exist with *N. pequopensis* in Nevada and has an range restricted to the upper "Baigendzhinian" (equivalent to uppermost Artinskian to lower Kungurian) (Ritter, 1986). Wang (2002) reported the occurrence of *Sw. variabilis* in this zone (in Bed 18). We have found morphotypes which are similar to *Sw. variabilis* but the specimens are not sufficiently

well-preserved to make an identification.

3) *Sw. asymmetrica* n. sp. Zone (41 – 76 m, Beds 18-25)

Lower limit: FAD of *Sw. asymmetrica* n. sp. Upper limit: FAD of *Neostreptognathodus prayi. Hindeodus catalanoi* and *Sw.* cf. *windi* co-occur in this zone. This Zone likely straddles the Artinskian-Kungurian boundary due to the absence of the *N. pnevi* Zone at Tieqiao.

4.3 Kungurian

Kungurian rocks, spanning Bed 25 to the lower part of Bed 109, consist mainly of medium-to-thick bedded fossiliferous pack- and grainstones with common chert nodules in the lower part. Medium to thin bedded lime mudstones and wackestones were gradually developed higher in the Kungurian strata, with a notable shift in fossil assemblages from a bryozoan- and calcareous algae-dominated shallow water facies (Beds 89-99) to a sponge spicule and radiolarian rich deeper water facies (Beds 100-111). In the latest Kungurian, conodont faunas change from *Hindeodus-Pseudohindeodus-Sweetognathus-*dominated and gondolellid-free assemblages to gondolellid-dominated assemblages (Bed 109). This shift coincides with a lithological change from thick- and medium- bedded wackestones to more cherty, medium- to thin- bedded wackestones and micritic mudstones.

The conodont biostratigraphy of the basal Kungurian Stage has been a matter of debate (Wang et al., 2011). Kozur et al. (1995) suggested the cline

Neostreptognathodus (N.) pequopensis-N. pnevi to be suitable for a definition for the Artinskian-Kungurian boundary. Mei et al. (2002) proposed the FAD of *N. pequopensis* or *Sw. guizhouensis* to define the base of the Kungurian whereas Chuvashov et al. (2002) formally proposed the FAD of *N. pnevi* as diagnostic of the base of the Kungurian, a definition that has been generally accepted (Henderson et al., 2012). However, due to the absence of *N. pnevi* at Tieqiao, we suggest alternatively using the FAD of *N. prayi* or *Sw. guizhouensis* to correlate the lower Kungurian. The Kungurian strata at Tieqiao is rather expanded (roughly 300 m thick) and is ideal for studying conodont zonation for this Stage. Six conodont zones have been established, described in ascending order below:

4) *Neostreptognathodus prayi* Zone (76 – 82.5 m, Beds 25-26)

Lower limit: FAD of *N. prayi*. Upper limit: FAD of *Sw. guizhouensis*. Benhken (1975) described the zonal element of *N. prayi* and illustrated a full growth series for the species. At Tieqiao, we recovered a few specimens which fit Behnken's (1975) description of the gerontic growth stage of *N. prayi* (Fig. 18 of Pl. 2 in Behnken, 1975; the same specimen is re-illustrated in Kozur, 1987). In addition, gerontic *N. prayi* and *Pseudosweetognathus costatus* can be easily differentiated due to their distinctive platform shoulders and different carina decorations.

The *N. prayi* Zone is the second oldest zone of the Kungurian in the standard Permian conodont zonation (Henderson et al., 2012) and so the *N. prayi* Zone at Tieqiao most probably does not indicate the "true" earliest Kungurian (Fig. 6). *Sw.*

clarki, a species most commonly seen in the late Artinskian (Beauchamp and Henderson, 1994), also extends to this zone.

5) *Sw. guizhouensis* Zone (82.5 – 260.5 m, Beds 26-66)

Lower limit: FAD of *Sw. guizhouensis.* Upper limit: FAD of *Sw. iranicus.* Except for in the lower part of this ~180 m thick conodont zone, conodonts are relatively rare. The long-ranging species *Pseudosweetognathus costatus* is the only species that was sparsely recovered in the upper part of this zone.

Sweetognathus guizhouensis is a cosmopolitan species that has high potential for supra-regional correlation. It is known from South China (Wang et al., 1987; Mei et al., 2002), Japan (Shen et al., 2012), and Sicily (Catalano et al., 1991), although it is not recorded in North America.

6) *Sw. iranicus* Zone (260.5 – 350 m, Beds 66-91)

Lower limit: FAD of *Sw. iranicus.* Upper limit: FAD of *Sw. subsymmetricus.* As with the *Sw. guizhouensis* Zone, both conodont diversity and abundance are very low. A major stratigraphic complication at this level of the section is that Beds 76-88 are a tectonic repetition of older beds (also see Sha et al., 1990).

7) *Sw. adjunctus* Zone (350 – 356 m, Bed 91)

Lower limit: FAD of *Sw. adjunctus.* Upper limit: FAD of *Sw. subsymmetrics.* *Sw. cf. paraguizhouensis* appears in this zone. Sha et al. (1990) reported the occurrence of *"Neogondolella" bisselli* in this zone (Bed 91). However, *"N". bisselli*

is an older species which often co-occurred with the Artinskian *Sw. whitei* group (e.g., Behnken, 1975; Clark et al., 1979; Orchard, 1984; Wang, 1994; Mei et al., 2002). The occurrence of *bisselli* obviously contradicts a Kungurian age of the host strata and also is not confirmed by our dataset.

Sw. adjunctus is also known from the uppermost Victorio Peak Formation from Texas and the upper Pequop Formation from Nevada, USA (Behnken, 1975) as well as from south-central British Columbia, Canada (Orchard and Forster, 1988): All of these occurrences are dated to be of late Leonardian age in the Permian regional stratigraphy (=middle to late Kungurian). Because of the geographically wide distribution of *Sw. adjunctus*, this zone therefore has high potential for super-regional correlation.

8) *Sw. subsymmetricus* Zone (356 – 393 m, Beds 91-99)

Lower limit: FAD of *Sw. subsymmetricus.* Upper limit: FAD of *Sw. hanzhongensis.* This zone correlates to the Kungurian "*M. siciliensis-Sw. subsymmetricus*" Zone in southern Guizhou (Mei et al., 2002).

Sw. subsymmetricus is well known from the Kungurian of Guizhou and Guangxi in South China, as well as from Thailand and Oman (Mei et al., 2002 and this study; Henderson and Mei, 2003; Metcalfe and Sone, 2008; Burrett et al., 2015). The report of the co-occurrence of *Sw. subsymmetricus* and *J. nankingensis* in the Nanjing area (Wang, 1995) suggests that the range of *Sw. subsymmetricus* extends at least to the earliest Roadian. However, the assertion that *Sw.*

subsymmetricus is only restricted to the Roadian (Kozur, 1993) is incorrect.

9) *Sw. hanzhongensis* Zone (393 – 454.5 m, Beds 99-109)

Lower limit: FAD of *Sw. hanzhongensis.* Upper limit: FAD of *M. idahoensis.* The FAD of *Pseudohindeodus augustus* and *Pseudohindeodus ramovsi* occurs in the middle part of this zone. A turnover in the dominant conodont fauna initiated during this zone. *Hindeodus* becomes abundant whilst the abundance and the diversity of *Sweetognathus* decreases. *Hindeodus permicus*, *H. gulloides* and *H. aff. wordensis* all occur in this zone.

4.4 Roadian

The Roadian strata consist of less than 15 m of weakly bioturbated but still finely laminated bedded micritic mudstones starting in Bed 109 (Fig. 2B). In Beds 110-111, strata are more thinly bedded with an increasing abundance of sponge spicules and radiolarian tests, indicating deepening and a relative sea level rise was ongoing throughout the Roadian. A major sea-level rise is known from the Early-Middle Permian transition and is manifest at Tieqiao by a transition to thinly bedded radiolarian cherts by Bed 112 (Wordian age). By this time, deep, basinal sedimentation was established in the region. The minor thickness of the Roadian strata may be attributed either to condensation during this sea level rise or to hiatus resulting in a loss of strata (due to sudden loss of carbonate production below the carbonate compensation depth). Only one conodont zone is recognised.

10) *Jinogondolella nankingensis* Zone (454.5– 468 m, Beds 109-111)

Lower limit: FAD of *J. nankingensis.* Upper limit: FAD of *J. aserrata. Pseudohindeodus ramovsi* are abundant. Disrupted lamination in the upper (Roadian) part of Bed 111 indicates weak bioturbation.

4.5 Wordian

Wordian strata are presented by Bed 112 to lowermost part of Bed 116. The sediments consist of thinly bedded radiolarian cherts in the lower part (Beds 112-113), thickly bedded bioclastic wacke- and packstones in the middle (Bed 114, also known as "the Great White Bed") and alternation of cherts and lime mudstones in the upper part (Bed 115-116). One conodont zone is recognised.

11) *J. aserrata* Zone (468– 588.5 m, Beds 112-116)

Lower limit: FAD of *J. aserrata*. Upper limit: FAD of *J. postserrata*. The FAD of *J. palmata* occurs at the same level as the FAD of *J. aserrata*. This is generally consistent with the record in west Texas where the FAD of *J. palmata* was reported very close to the FAD of *J. aserrata* (Nestell and Wardlaw, 2010a). Several species, such as *J. errata, Gullodus duani* and the long ranging species *Sw. hanzhongensis* and *Pseudohindeodus ramovsi* appear in the middle-upper part of this zone.

4.6 Capitanian

The Capitanian (Beds 116-119) is the most intensively studied interval in the

Laibin area (Mei et al., 1994c; Jin et al., 2006; Chen et al., 2009; Wignall et al., 2009b). Strata of this age consist of medium bedded alternating cherts and lime mudstones in the lower part (Beds 116-118) overlain by pack- to grainstones (Laibin Limestone Member, Bed 119). Here we only give a brief description of the conodont zones of this stage since they have been well studied.

12) *J. postserrata* Zone (588.5 – 593 m, Bed 116)

Lower limit: FAD of *J. postserrata*. Upper limit: FAD of *J. shannoni*.

13) *J. shannoni* Zone (593 – 596 m, Bed 116)

Lower limit: FAD of *J. shannoni*. Upper limit: FAD of *J. altudaensis*.

14) *J. altudaensis* Zone (596 – 664 m, Beds 116-117)

Lower limit: FAD of *J. altudaensis*. Upper limit: FAD of *J. prexuanhanensis*. This interval is characterised by extinctions amongst marine fauna and flora as well as the onset of Emeishan volcanism (Wignall et al., 2009a; Sun et al., 2010). Losses include many foraminifers, calcareous algae and brachiopods in the equatorial realm, and the latter also suffer comparable losses in the Boreal realm (Bond et al., 2010; Bond et al., 2015). Though there are no obvious lithological changes in the *J. altudaensis* Zone at Tieqiao, the last appearances of several long-ranging species, such as *Gullodus duani*, *Sw. hanzhongensis* and *Pseudohindeodus ramovsi*, are all recorded in this zone.

15) *J. prexuanhanensis* Zone (664 – 683.8 m, Beds 117-118)

Lower limit: FAD of *J. prexuanhanensis*. Upper limit: the FAD of *J. xuanhanensis*. This zone has not been recognised in western Texas (Lambert et al., 2002). However, it is distinguishable at Tieqiao (Guangxi, this study) and Dukou (Sichuan, Mei et al., 1994b). In condensed sections in Guizhou, *J. prexuanhanensis* zone is often combined with the younger *J. xuanhanensis* zone as the *J. prexuanhanensis-J. xuanhanensis* assemblage zone (Sun et al., 2010).

Sw. fengshanensis occurs in this zone. *Sw. fengshanensis* was established in the late Capitanian strata at Fengshan, northwestern Guangxi (Mei et al., 1998). In the Penglaitan section, *Sw. fengshanensis* spans the upper *J. postserrata* zone to the lower *J. xuanhanensis* zone, representing the last in the evolutionary lineage of sweetognathids in South China (Mei et al., 2002).

16) *J. xuanhanensis* Zone (683.8 – 697 m, Beds 118-119)

Lower limit: FAD of *J. xuanhanensis*. Upper limit: FAD of *J. granti*. Many mature morphotypes of *J. shannoni* occur in the lowermost part of this zone and are very similar to their counterparts from West Texas (Lambert et al., 2002; Wardlaw and Nestell, 2010). There is an influx of volcaniclastic material during this zone and it becomes more common in the overlying *J. granti* Zone, where it presumably derives from large scale explosive eruptions of the Emeishan Traps (Wignall et al., 2009b; Sun et al., 2010).

17) *J. granti* Zone (697 – 700 m, Bed 119)

Lower limit: FAD of *J. granti*. Upper limit: FAD of *Clarkina hongshuiensis*.

Conodonts are prolific in this zone with a typical yield rate of ~100 specimens per kg rock.

18) *Clarkina hongshuiensis* Zone (700 – 701.5 m, Bed 119)

Lower limit: FAD of *C. hongshuiensis*. Upper limit: FAD of *C. postbitteri*.

4.7 Wuchiapingian

The early Wuchiapingian (Bed 120) is characterised by deposition of extensive bedded cherts with intercalated pinkish limestone lenses. Evidence for a relative sea level fall towards the end of Wuchiapingian is indicated by a reduction of chert thickness up-section with carbonate sedimentation increasing. Eventually, this basinal setting evolved into a sponge reef facies in the later Wuchiapingian in which conodonts are barren. Two conodont zone are established for the earliest Wuchiapingian and the middle Wuchipingian:

19) *Clarkina postibitteri* Zone (701.5 – ? m, Bed 120)

Lower limit: FAD of *C. postbitteri*. Upper limit: not determined.

20) *Clarkina transcaucasica* Zone (Bed 134 and upward)

Lower limit: FO of *C. transcaucasica*. Upper limit: not determined.

Clarkina transcaucasica is found in Bed 134. Sha et al. (1990) reported the occurrence of *C. bitteri* in Bed 133. Although we cannot confirm this finding, *C. bitteri* occurs above the *C. asymmetrica* Zone and can extend to the *C. tanscaucasica* Zone (Jin and Shang, 2000) and so the observations of Sha et al.

(1990) are consistent with our interpretation.

The *C. transcaucasica* Zone at Tieqiao immediately overlies a sponge reef (Beds 123-133). The Wuchiapingian is known for paucity of reefs (Wang and Jin, 2000; Weidlich, 2002) and theTieqiao reef is one of just a handful of known Wuchiapingian reefs in South China. In terms of the standard zonation of Permian (Fig. 6), the Tieqiao reef can be constrained to the early to middle Wuchiapingian, possibly ranging from the *C. dukouensis* Zone to the *C. guangyuanensis* Zone.

5. Subordinate zones and reassessment for age assignments of rare species

Seven subordinate zones are established at Tieqiao, representing interval zones based on occurrences of long ranging species. The subordinate zones are less effective for stratigraphic correlation but can provide a valuable reference for cases when a single conodont assemblage is obtained from an age-ambiguous lithologic unit (e.g., Burrett et al., 2015).

In the following section, we first describe the ranges of these subordinate zones at Tieqiao, followed by comments on the ranges of the zonal species. A correlation with main conodont zones is shown in Figure 6. Note that the range of the species can be much longer than the respective zone.

1) *Pseudosweetognathus* (*Ps.*) *costatus* Interval Zone

Lower limit: FAD of *Ps. costatus.* Upper limit: FAD of *Ps. monocornus*. The *Ps. costatus* Zone spans the early Artinskian to middle Kungurian (Bed 19 to Bed 94).

Elements of long-ranging species *H. minutus* are abundant in the lower part of this zone and there is a single occurrence of *H.* aff. *catalanoi* in the lowermost.

Pseudosweetognathus costatus was established in Artinskian strata of South China (Wang et al., 1987) and also reported from Thailand, co-existing with a typical Kungurian taxon *Sw. subsymmetricus* (Metcalfe and Sone, 2008). Our data confirm former observations and indicate that the range of *Ps. costatus* extends from the Artinskian *Sw. asymmetrica* n. sp. Zone to the Kungurian *Sw. adjunctus* Zone. The *Ps. costatus-Ps. monocornus* lineage occurs as an anagenetic one at Tieqiao. In the middle Kungurian, *Ps. costatus* evolved into *Ps. monocornus*.

2) *Pseudosweetognathus monocornus* Interval Zone

Lower limit: FAD of *Ps. monocornus.* Upper limit: FAD of *H. gulloides*. This zone comprises Bed 94 to Bed 102 at Tieqiao, and is of late Kungurian age.

Li et al. (1989) established *Ps. monocornus* (under the genus "*Sichuanognathodus*") from the upper part of Maokou Fm. at Shangsi. A later, detailed study of the same section reported a *Jinogondolella* and *Hindeodus* dominated fauna which indicates an early Capitanian age for the upper Maokou Fm. (Sun et al., 2008).

Pseudosweetognathus monocornus is found in the upper part of Chihsia Fm. and lower part of Maokou Fm. at Tieqiao and here is reassigned a middle-Kungurian to early-Roadian age. This species only occurred in a shallow water, high energy assemblage composed of calcareous algae, corals and

foraminifers found in thickly bedded bioclastic pack- and grainstones (e.g., in Bed 114, the Great White Bed). We thus speculate that the occurrence of *Ps. monocornus* might be facies-related, and its presence in Wordian to lower Capitanian strata elsewhere (Li et al., 1989) cannot be excluded.

Pseudosweetognathus monocornus superficially resembles gerontic morphotypes of *N. prayi* (fig. 8, Pl.2; also see fig. 18 of Pl. 2 in Behnken, 1975). The main differences between the two species are the shapes of the platform shoulders and carina ornaments. However, taxonomical discussion on these two species is beyond the scope of this paper.

3) *Hindeodus gulloides* Interval Zone

Lower limit: FAD of *H. gulloides*. Upper limit: FAD of *Pseudohindeodus (Ph.) ramovsi*. This zone occupies Bed 102 and correlates to the middle part of *Sw. hanzhongensis* Zone, representing a Late Kungurian age.

The species *H. gulloides* Kozur and Mostler, 1995, ranges from upper Kungurian to Roadian. In northeast Thailand, *H. gulloides* occurs at an age-equivalent level as in South China and co-existed with a typical late Kungurian assemblage which consists of species *Mesogondolella siciliensis, Ph. oertlii* (= *angustus*? our brackets) and *Sw. subsymmetricus* (Burrett et al., 2015). In west Texas, the species was recovered from the upper part of Road Canyon Fm., representing a late Roadian age (Kozur and Mostler, 1995).

4) *Pseudohindeodus ramovsi* Interval Zone

Lower limit: the FAD of *Ph. ramovsi*. Upper limit: the occurrence of *Gullodus sicilianus*. This zone spans from Bed 103 to Bed 115, representing a latest Kungurian to Wordian age.

The species *Ph. ramovsi* Gullo and Kozur, 1992 has a much longer range than the Interval Zone. Wardlaw (2000) reported sporadic occurrences of this species from the Kungurian to Capitanian. Our data are consistent with Wardlaw (2000), suggesting that *Ph. ramovsi* spanned from the late Kungurian *Sw. hanzhongensis* Zone to the middle Capitanian *J. altudaensis* Zone.

Another associate species in this zone is *Ph. augustus* (Igo, 1981). This species has been reported from coeval Kungurian strata in Japan (Igo, 1981; Shen et al., 2012), but can also occur in much older strata such as in the Artinskian (Orchard and Forster, 1988).

5) *Gullodus sicilianus* Interval Zone

Lower limit: FO of *G. sicilianus.* Upper limit: FAD of *Gullodus duani*. This zone covers the middle part of Bed 115, representing a middle-late Wordian age.

Gullodus sicilianus (Bender and Stoppel, 1965) ranges from the Roadian to Wordian (Kozur, 1993). It is a rare taxon that is known mostly from the Tethys realm during the Wordian (Kozur, 1995).

6) *Gullodus duani* Interval Zone

Lower limit: FAD of *Gullodus duani*. Upper limit: prolific occurrence of *H.*

excavatus. This zone comprises Bed 115 to Bed 118, and includes much of the Capitanian strata.

Gullodus duani Mei et al. 2002 is a rather rare species in the Guadalupian. This species was originally recovered from the Maokou Fm. from Guangxi and is only known from South China. At Tieqiao, this species is known from uppermost Wordian to middle Capitanian strata.

An associated taxon *Hindeodus catalanoi* ranges through the upper part of this zone. Though Gullo and Kozur (1992) assigned a Wordian age for *H. catalanoi*, this form is found in the Capitanian at Tieqiao, suggesting a longer range of the species than its original definition.

7) *Hindeodus excavatus* Interval Zone

Lower limit: the prolific occurrence of *H. excavatus.* Upper limit: FAD of *C. postbitteri* (the Capitanian-Wuchiapingian boundary). At Tieqiao, this zone is represented by the Laibin Limestone Member (Bed 119) of late Capitanian age.

Hindeodus excavatus is another long-ranging species in the Permian, but its use as a zonal fossil derives from its prolific abundance in the late Capitanian.

6. Systematic palaeontology

Genus ***Gullodus* Kozur, 1993**

Emended diagnosis: Spathognathodiform elements with a medium to long anterior blade and a posteriorly positioned, strongly expanded basal cavity.

Denticles occur on the blade and above the basal cavity and are in most cases without ornamentations. Denticles are generally 10-18 in number and those above the basal cavity can be expanded and form a carina-like structure or narrow transverse ridges. Small coalesced denticles are sometimes developed on the anterior edge forming an "anterior blade". Length/height ratio is between 1.5 and 3. Basal cavities are expanded, non-ornamented and occupy 1/3 to 2/3 of the full body.

Remarks: the diagnosis of this genus (Kozur, 1993) should be emended because it is often hard to differentiate between *Gullodus* and *Hindeodus*. The emended diagnosis also includes wider variability of *Gullodus* species. Basal cavities of *Gullodus* are more expanded than most *Hindeodus* species but not as greatly expanded as *Pseudohindeodus*. Key differences between *Gullodus* and *Hindeodus* are the shape and position of the basal cavity and the length/height ratio: *Hindeodus* has a more centrally positioned basal cavity and lower length/height ratio. A key difference between *Gullodus* and *Sweetognathus* is that denticles of *Gullodus* are not ornamented while those of *Sweetognathus* develop pustules. *Gullodus* can be differentiated from *Pseudohindeodus* because the basal cavity of the latter is more horizontally expanded and ornamented with a surface apron (i.e., a crimp around the fringe of the basal cavity) and occupies ≥2/3 of the full element length.

Based on the revised diagnosis, *Gnathodus sicilianus* Bender and Stoppel, 1965 should remain as *Gullodus sicilianus* as suggested by Kozur (1993).

However, *Pseudohindeodus catalanoi* Gullo and Kozur (1992) and *Gullodus hemicircularis* Kozur, 1993 should be assigned to *Hindeodus*, rather than *Pseudohindeodus* or *Gullodus*.

Occurrence: Kungurian to Capitanian

Gullodus tieqiaoensis n. sp. Sun and Lai

Plate 4, figs. 6, 7.

No reported specimens are similar to this species.

Etymology: From the name of the section from where the species is described.

Holotype: Specimen S1_060 (Pl. 4, fig.6) from sample 41-1 of Bed 41, Chihsia Fm., Tieqiao Section, South China.

Paratype: Specimen S1_062 (Pl. 4, fig.7) from sample 41-2 of Bed 41, Chihsia Fm., Tieqiao Section, South China.

Type locality: specimens were obtained from Bed 40 to 44 in the lower Chihsia Fm., Tieqiao, South China.

Type interval: lower *Sw. guizhouensis* Zone, early Kungurian.

Diagnosis: A *Gullodus* species with a high length/height ratio of ~2 and a robust cusp.

Description: Body slim and elongated. Length/height ratio is ~2. The cusp is

erected, tall, wide and robust, normally twice as high as the denticles and three times wider than the denticles. 13-17 densely arranged denticles decease in height posteriorly. Posterior denticles above the basal cavity are more expanded and thus wider than the rest. They can be lower and more fused. The basal cavity is expanded, leaf or irregular shaped and occupies the posterior 2/3 of the element. The widest point is in the posterior 1/4 to 1/3.

Remarks: This species has a very high length/height ratio and a posteriorly positioned, expanded but non-ornamented basal cavity that extends to the posterior end. It thus belongs to *Gullodus* rather than *Hindeodus* or *Pseudohindeodus*.

Occurrence: lower Chihsia Fm. (early Kungurian), Tieqiao, South China

Genus *Hindeodus* Rexroad & Furnish, 1964

Hindeodus catalanoi Gullo and Kozur, 1992

Plate 7, Figs. 6-8.

Pseudohindeodus catalanoi n. sp. Gullo and Kozur, 1992 p. 225, pl. 5, fig. A.

Hindeodus gulloides Kozur and Mosher, 1995; Burrett et al. 2015, p. 111-113, Fig. 6, figs. J-I.

Diagnosis: A *Hindeodus* species that is triangular shaped (in lateral view) with 2 to 3 anterior coalesced denticles and 12-15 densely arrayed denticles.

Remarks: The species resembles its Artinskian-Kungurian and "Roadian" predecessors *H. hemicircularis* Kozur 1993 and *H. gulloides* Kozur and Mostler, 1995. They all have two to three anterior denticles. However, *H. hemicircularis* is sub-semicircular shaped and has fewer but wider denticles while *H. gulloides* is more elongated and has a much broader cusp than the current species.

H. catalanoi was previously known only from the Wordian of Sicily (Gullo and Kozur, 1992). Our collections from Tieqiao extend the range of the species to the *J. altudaensis* zone of middle Capitanian.

Occurrence: upper Maokou Fm. (middle-late Capitanian), Tieqiao, South China; Wordian of Sicily.

Hindeodus sp. A

Plate 4, Figs. 23, 26.

Diagnosis: A *Hindeodus* species whose outline is close to that of an isosceles triangle.

Description: Body triangular shaped (lateral view) with a long anterior edge. Anterior angle is around 45˚-60˚. Two or three small coalesced denticles may develop on the anterior edge. Medium sized cusp followed by three low denticles. Posterior denticles are taller and wider and decrease in height towards the posterior end. The basal cavity is medially expanded and central positioned.

Remarks: The species resembles *H. permicus* but differs by its outline and shapes

of denticles.

Occurrence: upper Kungurian, basal Maokou Fm. of South China

Genus *Pseudohindeodus* **Gullo and Kozur, 1992**

Pseudohindeodus elliptica **n. sp. Sun and Lai**

Plate 4, fig. 13; Plate 7. fig. 14.

Pseudohindeodus sp. Wang, 1995, pl. 1, figs. 1a, 1b.

Etymology: From the oval shape of the basal cavity of the species.

Holotype: Specimen S7_001 (Pl. 7, fig. 14) from sample 104-2 of Bed 104, Maokou Fm., Tieqiao Section, South China.

Paratype: Specimen S2_075 (Pl. 4, fig. 13) from sample 104-2 of Bed 104, Maokou Fm., Tieqiao Section, South China.

Type locality: specimens were obtained from Bed 104 in the lower Maokou Fm., Tieqiao, South China.

Type interval: Sw. hanzhongensis Zone to *J. nankingensis* Zone; late Kungurian to Roadian.

Diagnosis: A *Gullodus* species with an asymmetrical basal cavity that is near oval in shape.

Description: Element is small and rounded. Cusp is large, robust and higher and broader than any following denticles. The 5-8 denticles immediately behind the

cusp are thin and more fused with each other and thus can appear as a ridge. The last 4-6 denticles are the largest amongst all denticles. They are lower, more rounded in shape and relatively evenly spaced with each other with a small gap in between. The basal cavity is decorated with a surface apron, horizontally expanded, asymmetrical and very rounded. The outline of the basal cavity is close to an oval.

Remarks: the species resembles *Ph. ramovsi*. However, *ramovsi* has a near triangular basal cavity whilst *Ph. elliptica* n. sp. has a more rounded basal cavity.

The *Ph.* sp. reported by Wang (1995) is assigned to *Ph. elliptica* n. sp. It co-occurs with Roadian element *J. nankingensis* at Longtan, Nanjing area (Wang, 1995).

Occurrence: basal Kufeng Fm. and lower Maokou Fm. of South China.

<div align="center">

Genus *Sweetognathus* **Clark, 1972**

Sweetognathus asymmetrica **n. sp. Sun and Lai**

Plate 1, Figs. 1, 7, 14, 17.

</div>

Sweetognathus sp. Chernykh, 2006 pl. XIII, figs. 1, 2.

Etymology: The species name refers to its asymmetric anterior transverse ridges.

Holotype: Specimen S1_018 (Pl. 1, Fig.1) from sample 18-1 of Bed 18, Chihsia Fm., Tieqiao Section, South China.

Paratypes: Specimen S1_037 (Pl. 1, Fig.7) from sample 22-2 of Bed 22, Chihsia

Fm., Tieqiao Section, South China.

Type locality: specimens were obtained from Beds 18 to 24 in the lower Chihsia Fm., Tieqiao, South China

Type interval: middle Artinskian to the earliest Kungurian

Diagnosis: A Type III sweetognathid (definition follows Ritter, 1986) with short blade and asymmetric anterior transverse ridges.

Description: Short blade, often bearing 4-6 denticles; the first anterior blade denticle is moderately big. The second denticle is the biggest and very often fused with the first denticle and forms a high robust denticle; the other denticles are much smaller, lower and more fused toward to the carina. The first two denticles are occasionally both very high, robust and triangular in shape. Transverse ridges are clearly incised. There are commonly 6 to 8 transverse ridges. The first one or two ridges are always asymmetrically developed—in most cases the left ridges are missing. The widest part of the carina is in the middle. The basal cavity is leaf- to heart-shaped and moderately expanded, occupying the posterior half of the full element length.

Remarks: This species is similar to *Sw. subsymmetricus.* Both species developed asymmetric anterior transverse ridges. However, the current species differs from *Sw. subsymmetricus* by: 1) the length ratio of free blade/carina < 1 (most commonly 1/2 to 1/4), whereas that of *Sw. subsymmetricus* generally ranges from 1/2 to ≥1; 2) the first denticle on the anterior blade is large, tall and robust,

whereas that of *Sw. subsymmetricus* is moderately large, compared with other denticles on the blade; 3) an apparent low ridge between blade and carina; *Sw. subsymmetricus* has small and low denticles connecting blade and carina; 4) *Sw. subsymmetricus* has a less expanded basal cavity and a narrower carina, therefore appears more "slim"; 5) gaps between transverse ridges are more or less evenly spaced, whereas those of *Sw. subsymmetricus* become lager toward the posterior end.

Though *Sw. subsymmetricus* and *Sw. asymmetrica* n. sp. may have close affinities, *Sw. asymmetrica* n. sp. is restricted to the Artinskian to earliest Kungurian whereas *Sw. subsymmetricus* is found in younger rocks of late Kungurian to Roadian age (Kozur, 1995). Many reported occurrences of *Sw. subsymmetricus* in pre-middle-Kungurian strata (most of which have not been illustrated) should be reassessed.

The paratype shares a few common features with *Sw. variabilis*. They both have two big triangular-shaped denticles on the blade. The key difference is the position of the basal cavity. *Sw. variabilis* has a basal cavity near the posterior end. In addition, *Sw. variabilis* has a long blade (blade/carina ratio ≥1) and five transverse ridges with the widest being near the posterior end. *Sw. asymmetrica* n. sp. has a blade/carina ratio always <1, and usually seven or more transverse ridges while the widest occurs near the middle of the body. In addition, *Sw. subsymmetricus* and *Sw. variabilis* are rather distinctive species and should preferably not be considered as synonyms of *Sw. paraguizhouensis* and *Sw.*

guizhouensis (Shen et al., 2012).

Figures 1, 2 on Plate XIII in Chernykh (2006) are both from the Bursevian horizon in the lower Artinskian *Sw. whitei* Zone and are assigned to *Sw. asymmetrica* n. sp.

Note: The specimen shown in fig. 3 in Pl. 4 seemly has a gap between blade and carina. This is an artefact of photography.

Sweetognathus bogoslovskajae

Pl. 1, fig. 11; Pl. 2, figs. 1, 2, 4, 9.

Sweetognathus bogoslovskajae n. sp. Kozur; Kozur and Mostler, 1976, p. 18-19, pl. 3, fig. 7, 8.

Sweetognathus whitei (Rhodes, 1963); Kang et al., 1987, pl. IV, figs. 12, 14.

Sweetognathus bogoslovskajae Kozur; Mei et al., 2002, Fig. 12.5; Fig. 10.13.

Remarks: The current species has a slim carina. The maximum width is uniquely in the front third to the middle of the carina. A gap likely develops between the blade and the carina. The node-like denticles on the carina rarely develop into broad transverse ridges and are widely spaced.Such space between denticles increases towards the posterior end.

Sweetognathus hanzhongensis (Wang, 1978)

Pl. 3, figs. 15-18; Pl. 7, figs. 9-10.

Gnathodus hanzhongensis n. sp. Wang, 1978, p. 217, pl. I, figs. 33-35, 40-41.

Sweetognathus hanzhongensis (Wang), Wang and Dong, 1991, pl. III, figs. 6-8.

Sweetognathus iranicus hanzhongensis (Wang, 1978), Mei et al., 2002, p. 85, Fig. 10, figs. 6-7 (only).

Description (direct translation from Wang, 1978): the element consists of a near-rectangular blade (if viewed laterally) and a relatively elongated, two way pointed ovate basal cap. The front edge of the blade is almost vertical and forms a right anterior angle together with the lower edge. The blade is of 1/3 of the full element in length and consists of 4-6 fused denticles. The basal cavity is thin and is of 2/3 of the element length. The maximal width is near the middle or slightly in front. The lower edge (of the basal cavity, our brackets) is often broken due to incomplete preservation. The basal cavity is empty inside and unornamented on the surface. A moderately high carina is developed in the middle and is composed of almost completely fused denticles (i.e., node-like denticles with pustulose ornamentations, our brackets). The carina has a smooth upper outline.

Remarks: Specimens illustrated in Wang (1978) each have 4-6 denticles on the blade and the first three (in one case four) denticles are about the same size, and larger than thelater denticles. In one specimen (Pl. I, fig. 35 in Wang, 1978), the second anterior blade denticle is the largest. One of the key features of this species is that the fused node-like denticles form a smooth middle carina (lateral view) and this smooth part extends at least to the middle of the basal cavity and

occasionally to near the posterior end (e.g., Pl. I, fig. 33 in Wang, 1978).

Sweetognathus inornatus Ritter, 1986

Pl. 1, figs. 10; Pl. 7, fig. 2.

Sweetognathus whitei (Rhodes, 1963); Clark et al., 1979, pl. 1, fig. 15.

Sweetognathus aff. *whitei* (Rhodes, 1963); Orchard, 1984, p. 213, pl. 23.1 figs. 1?, 2.

Sweetognathus inornatus n. sp. Ritter, 1986, p. 150, pl. 3, figs. 1, 6-7, 12-15; pl. 4, figs. 2, 9, 13, 14.

Remarks: Mei et al. (2002) considered the current species to be a synonym of *Sw. whitei* whilst Boardman et al. (2009) considered it to be a synonym of older *Sw. anceps*. We emphasise that *Sw. inornatus* is a distinct species. A key feature of the current species is that 2 to 3 slim denticles are often partially or completely merged together to form a short ridge connecting the blade and the carina. Neither *Sw. whitei* nor *Sw. anceps* has this feature*.*

The current species is very similar to *Sw. iranicus* in outline. However, the maximum width of the current species is in the middle of the carina whist the carina of *Sw. iranicus* increases in width posteriorly and the maximum width is near the posterior 1/3 to 1/4. Denticles between the blade and the carina of *Sw. iranicus* are low and merged together to form a gap, not a higher ridge as in *Sw. inornatus*.

Sweetognathus sp. A

Pl. 1, fig. 9.

Diagnosis: A Type III sweetognathid with tall and slim denticles and narrow ridges.

Description: Body elongated with a height/length ratio $\approx 1/2$. The first anterior blade denticle is tall and slim, at least twice as high as any following denticles, and is immediately followed by five to six very slim denticles. The second and fourth denticles are the lowest. A gap is developed between the fifth and sixth denticles. Pustules are short, forming 5-7 low and generally evenly spaced ridges.

Sweetognathus toriyamai (Igo, 1981)

Pl. 1, figs. 12, 15.

Neostreptognathodus toriyamai n. sp. Igo, 1981, p. 42-43, pl. 6, figs. 1-16

Sweetognathus whitei (Rhodes, 1963) Igo, 1981, pl. 7, fig.7?

Remarks: The denticles on the anterior blade of this species point forwards. The carina is lens-shaped—thus the widest is near the middle. There is a short and narrow ridge connecting the blade and carina. The ridge is relatively high anteriorly and decreases in height posteriorly towards the carina, thus giving a triangular shape if laterally viewed.

Comparisons: The short narrow ridge between the free blade and carina is one of the most distinguishable features of this species. The current species and *Sw. behnkeni* both have a broad, lens-like carina with a maximum width in the middle.

However, the latter species has "ledge-like" decorations on the carina, whereas *Sw. toriyamai* is decorated by lower transverse ridges.

Occurrence: Artinskian, basal Chihsia Fm. of South China and Kuchibora Fm. of Japan.

7. Conclusions

A detailed conodont biostratigraphic and taxonomic study of the Permian strata at Tieqiao, South China has enabled recognition of 20 main and 7 subordinate conodont zones from the Artinskian stage to the Wuchiapingian stage. Three new species are established. The following conclusions can be drawn:

1) The Tieqiao strata record a change in conodont faunas from Early Permian *Sweetognathus* dominated assemblages to Middle Permian gondolellids dominated assemblages from the latest Kungurian onwards. This shift coincided with a relative sea-level rise and change to deeper water facies.

2) The Early Permian *Sweetognathus* fauna represents an important evolutionary lineage and a shallower (surface?) water group, which evolved in parallel to the contemporary but possibly deeper-dwelling *Mesogondolella* fauna.

3) The Chihsia Fm., which had been in many cases erroneously regarded as a Middle Permian unit, is of Early Permian age. It spans the Artinskian to the late

Kungurian whilst the overlying Maokou Fm. straddles the Early and Middle Permian from the late Kungurian to latest Capitanian. The Chihsia/Maokou lithological boundary is thus locally not suitable for defining the Early-Middle Permian boundary (Kungurian-Roadian stage boundary).

4) Species such as *J. palmata* and *J. errata* occur at time-equivalent stratigraphic levels at Tieqiao as in west Texas, suggesting that they can be used for intercontinental correlations.

5) Our conodont biozones constrain the age of the Late Permian sponge reef at Tieqiao to the early and middle Wuchiapingian (from the *C. dukouensis* zone to *C. guangyuanensis* zone).

Acknowledgements

References

Beauchamp, B., Henderson, C.M., 1994. The Lower Permian Raanes, Great Bear Cape and Trappers Cove Formations, Sverdrup Basin, Canadian Arctic - Stratigraphy and Conodont Zonations. Bulletin of Canadian Petroleum Geology, 42(4): 562-597.

Behnken, F.H., 1975. Leonardian and Guadalupian (Permian) Conodont Biostratigraphy in Western and Southwestern United States. Journal of Paleontology, 49(2): 284-315.

Bender, H., Stoppel, D., 1965. Perm-Conodonten. Geologisches Jahrbuch, 82: 331-364.

Boardman, D.R., Wardlaw, B.R., Nestell, M.K., 2009. Stratigraphy and Conodont Biostratigraphy of the Uppermost Carboniferous and Lower Permian from the North American Midcontinent. Kansas Geological Survey Bulletin, 255: 1-130.

Bond, D.P.G. et al., 2010. The Middle Permian (Capitanian) mass extinction on land and in the oceans. Earth-Science Reviews, 102(1-2): 100-116.

Bond, D.P.G. et al., 2015. An abrupt extinction in the Middle Permian (Capitanian) of the Boreal Realm (Spitsbergen) and its link to anoxia and acidification. Geological Society of America Bulletin, 127(9-10): 1411-1421.

Bucur, I.I., Munnecke, A., Granier, B., Yan, J., 2009. Remarks on the Permian dasycladalean alga Sinoporella leei Yabe, 1949. Geobios, 42(2): 221-231.

Burrett, C., Udchachon, M., Thassanapak, H., Chitnarin, A., 2015. Conodonts, radiolarians and ostracodes in the Permian E-Lert Formation, Loei Fold Belt, Indochina Terrane, Thailand. Geological Magazine, 152(01): 106-142.

Catalano, R., Di Stefano, P., Kozur, H., 1991. Permian circumpacific deep-water faunas from the western Tethys (Sicily, Italy)—new evidences for the position of the Permian Tethys. Palaeogeography, Palaeoclimatology, Palaeoecology, 87(1–4): 75-108.

Chen, B., Joachimski, M.M., Sun, Y.D., Shen, S.Z., Lai, X.L., 2011. Carbon and conodont apatite oxygen isotope records of Guadalupian-Lopingian boundary sections: Climatic or sea-level signal? Palaeogeography Palaeoclimatology Palaeoecology, 311(3-4): 145-153.

Chen, Z.Q., George, A., Yang, W.R., 2009. Effects of Middle-Late Permian sea-level changes and mass extinction on the formation of the Tieqiao skeletal mound in the Laibin area, South China. Australian Journal of Earth Sciences, 56(6): 745-763.

Chernykh, V.V., 2005. Zonal method in biostratigraphy, zonal conodont scale of the Lower Permian in the Urals. Institute of Geology and Geochemistry of RAN, Ekaterinburg, 217 pp.

Chuvashov, B.I., Dyupina, G.V., Mizens, G.A., Chernykh, V.V., 1990. Basic Sections of Carboniferous and Lower Permian of Western Slope of Urals. Ural Branch Academic Science of Russia, Sverdlovsk, 369 pp.

Clark, D.L., Behnken, F.H., 1971. Conodonts and Biostratigraphy of the Permian. Geological Society of America Memoir, 127: 415-439.

Clark, D.L., Carr, T.R., Behnken, F.H., Wardlaw, B.R., Collinson, J.W., 1979. Permian Conodont Biostratigraphy in the Great Basin. In: Sandberg, C.A., Clark, D.L. (Eds.), Conodont biostratigraphy of the Great Basin and Rocky Mountains. Brigham Young University, Geology Studies, pp. 143-150.

Ding, H., Wan, S., 1990. The Carboniferous-Permian conodont event-stratigraphy in the South of the North China Platform. Courier Forschungsinstitut Senckenberg, 118: 131-155.

Gong, Y.-M., Shi, G.R., Zhang, L.-J., Weldon, E.A., 2010. *Zoophycos* composite ichnofabrics and tiers from the Permian neritic facies in South China and south-eastern Australia. Lethaia, 43(2): 182-196.

Gullo, M., Kozur, H., 1992. Conodonts from the pelagic deep-water Permian of central Western-Sicily (Italy). Neues Jahrbuch für Geologie und Paläontologie Abhandlungen, 184(2): 203-234.

Henderson, C.M., Davydov, D.I., Wardlaw, B.R., 2012. The Permian Period. In: Gradstein, F.M., Ogg, J.G., Schmitz, M.D., Ogg, G.M. (Eds.), The Geologic Time Scale 2012. Elsevier, pp. 653-679.

Henderson, C.M., Mei, S., 2003. Stratigraphic versus environmental significance of Permian serrated conodonts around the Cisuralian-Guadalupian boundary: new evidence from Oman. Palaeogeography, Palaeoclimatology, Palaeoecology, 191(3-4): 301-328.

Henderson, C.M., Mei, S., Wardlaw, B.R., 2002. New conodont definitions at the Guadalupian-Lopingian boundary. In: Hills, L.V., Henderson, C.M., Bamber, E.W. (Editors), Carboniferous and Permian of the world. Memoir - Canadian Society of Petroleum Geologists, pp. 725-735.

Igo, H., 1981. Permian conodont biostratigraphy of Japan. Palaeontological Society of Japan special papers, 24. Palaeontological Society of Japan, Tokyo, 51 pp.

Ji, Z.S. et al., 2004. Early Permian Conodonts from the Baoshan Block, Western Yunnan, China. Acta Geologica Sinica, 78(6): 1179-1184.

Jiang, H.S. et al., 2007. Restudy of conodont zonation and evolution across the P/T boundary at Meishan section, Changxing, Zhejiang, China. Global and Planetary Change, 55: 39-55.

Jin, Y. et al., 2006. The Global Stratotype Section and Point (GSSP) for the boundary between the Capitanian and Wuchiapingian Stage (Permian). Episodes, 29(4): 253-262.

Jin, Y., Wardlaw, B.R., Glenister, B.F., Kotlyar, G.V., 1997. Permian chronostratigraphic subdivisions. Episodes, 20(1): 10-15.

Jin, Y.G., Shang, Q.H., 2000. The Permian of China and its interregional correlation. In: Yin, H.F., Dickins, J.M., Shi, G.R., Tong, J.N. (Eds.), Permo-Triassic evolution of Tethys and Western Circum-Pacific. Elsevier, pp. 71- 98.

Kozur, H., 1987. Beiträge zur Stratigraphie des Perms Teil II: Die Conodontenchronolgie des Perms.

Freiberger Forschungsheft, 334: 85-161.

Kozur, H., 1993. Gullodus n. gen.–a new conodont genus and remarks to the pelagic Permian and Triassic of Western Sicily. Jb. Geol. B. -A., 136(1): 77-87.

Kozur, H., 1995. Permian Conodont Zonation and its Importance for the Permian Stratigraphic Standard Scale. Geol. Palaont. Mitt. Innsbruck, 20(165-205).

Kozur, H., Mostler, H., 1995. Guadalupian (Middle Permian) conodonts of sponge-bearing limestones from the margins of the Delaware Basin, West Texas. Geologia Croatica, 48(2): 107-128.

Lambert, L.L., Gorden L. Bell, J., Fronimos, J.A., Wardlaw, B.R., O.Yisa, M., 2010. Conodont biostratigraphy of a more complete Reef Trail Member section near the type section, latest Guadalupian Series type region. Micropaleontology, 56(1-2): 233-253.

Lambert, L.L., Wardlaw, B.R., Nestell, M.K., Nestell, G.P., 2002. Latest Guadalupian (Middle Permian) conodonts and foraminifers from West Texas. Micropaleontology, 48(4): 343-364.

Li, Z.S. et al., 1989. Study on the Permian-Triassic biostratigraphy and event stratigraphy of northern Sichuan and southern Shaanxi. Geological Memoirs, 9. Geological Publishing House, Beijing, 435 pp.

Mei, S., Jin, Y., Wardlaw, B.R., 1994a. Succession of Wuchiapingian conodonts from northeast Sichuan Province and its worldwide correlation. Acta Micropalaeontologica Sinica, 11: 121-139.

Mei, S., Jin, Y.G., Wardlaw, B.R., 1994b. Succession of conodont zones from the Permian 'Kuhfeng' Formation, Xuanhan, Sichuan and its implication in global correlation. Acta Palaeontologica Sinica, 33(1): 1-23.

Mei, S.L., Henderson, C.M., Wardlaw, B.R., 2002. Evolution and distribution of the conodonts *Sweetognathus* and *Iranognathus* and related genera during the Permian, and their implications for climate change. Palaeogeography, Palaeoclimatology, Palaeoecology, 180(1-3): 57-91.

Mei, S.L., Jin, Y.G., Wardlaw, B.R., 1994c. Zonation of conodonts from the Maokouan-Wuchiapingian boundary strata, South China. Palaeoworld, 4: 225-233.

Mei, S.L., Jin, Y.G., Wardlaw, B.R., 1998. Conodont Succession of the Guadalupian-Lopingian Boundary Strata in Laibin of Guangxi, China and West Texas, USA. Palaeoworld, 9: 53-76.

Metcalfe, I., Sone, M., 2008. Biostratigraphy and palaeobiogeography of Lower Permian (lower Kungurian) conodonts from the Tak Fa Formation (Saraburi Limestone), Thailand. Palaeogeography, Palaeoclimatology, Palaeoecology, 257(1-2): 139-151.

Nestell, M.K., Nestell, G.P., Wardlaw, B.R., Sweatt, M.J., 2006. Integrated biostratigraphy of foraminifers, radiolarians and conodonts in shallow and deep water Middle Permian (Capitanian) deposits of the "Rader slide", Guadalupe Mountain, West Texas. Stratigraphy, 3(3): 161-194.

Nestell, M.K., Wardlaw, B.R., 2010a. *Jinogondolella palmata*, a new Gondolellid conodont species from the Bell Canyon Formation, Middle Permian, West Texas. Micropaleontology, 56(1-2): 185-194.

Nestell, M.K., Wardlaw, B.R., 2010b. Radiolarians and conodonts of the Guadalupian (Middle Permian) of West Texas: advances in taxonomy and biostratigraphy. Micropaleontology, 56(1-2): 1-6.

Orchard, M.J., 1984. Early Permian conodonts from the Harper Ranch beds, Kamloops area, southern British Columbia. Paper - Geological Survey of Canada, 84-1B: 207-215.

Orchard, M.J., Forster, P.J.L., 1988. Permian Conodont Biostratigraphy of the Harper Ranch Beds, Near Kamloops, South-central British Columbia. Energy, Mines and Resources Canada, pp.

1-27.

Qiu, Z., Wang, Q., Zou, C., Yan, D., Wei, H., 2013. Transgressive–regressive sequences on the slope of an isolated carbonate platform (Middle–Late Permian, Laibin, South China). Facies: 1-19.

Rhodes, F.H., 1963. Conodont from the topmost Tensleep Sandstone of the eastern Big Norn Mountains, Wyoming. Journal of Paleontology, 37: 401-408.

Ritter, S.M., 1986. Taxonomic revision and phylogeny of post-Early Permian crisis *bisselli-whitei* Zone conodonts with comments on late Paleozoic diversity. Geologica et Palaeontologica, 20: 139-165.

Sha, Q.A., Wu, S.W., Fu, J.M., 1990. An integrated investigation on the Permian System of Qin-Gui areas, with discussion on hydrocarbon potential. Science Press, Beijing, 252 pp.

Shen, S.-Z., Wang, Y., Henderson, C.M., Cao, C.-Q., Wang, W., 2007. Biostratigraphy and lithofacies of the Permian System in the Laibin-Heshan area of Guangxi, South China. Palaeoworld, 16(1-3): 120-139.

Shen, S.-z., Yuan, D.-x., Henderson, C.M., Tazawa, J., Zhang, Y.-c., 2012. Implications of Kungurian (Early Permian) conodonts from Hatahoko, Japan, for correlation between the Tethyan and international timescales. Micropaleontology, 58(6): 505-522.

Sheng, J.Z., Jin, Y.G., 1994. Correlation of Permian deposits of China. Palaeoworld, 4: 14-113.

Sun, Y.D. et al., 2008. Guadalupian (Middle Permian) Conodont Faunas at Shangsi Section, Northeast Sichuan Province. Journal of China University of Geosciences, 19(5): 451-460.

Sun, Y.D. et al., 2010. Dating the onset and nature of the Middle Permian Emeishan large igneous province eruptions in SW China using conodont biostratigraphy and its bearing on mantle plume uplift models. Lithos, 119(1-2): 20-33.

Wang, C.Y., 1995. A conodont fauna from the lowermost Kufeng Formation (Permian). Acta Micropalaeontologica Sinica, 12(3): 293-297.

Wang, C.Y., 2002. Permian conodonts from Laibin and Heshan, Guangxi. Bulletin of Nanjing Institute of Geology and Palaeontology, Acdemia Sinica, 15: 180-190.

Wang, C.Y., Ritter, S.M., Clark, D.L., 1987. The *Sweetognathus* complex in the Permian of China: implications for evolution and homeomorphy. Journal of Paleontology, 61: 1047-1057.

Wang, D., Jiang, H., Gu, S., Yan, J., 2016. Cisuralian–Guadalupian conodont sequence from the Shaiwa section, Ziyun, Guizhou, South China. Palaeogeography, Palaeoclimatology, Palaeoecology, 457: 1-22.

Wang, W., Cao, C.Q., Wang, Y., 2004. The carbon isotope excursion on GSSP candidate section of Lopingian-Guadalupian boundary. Earth and Planetary Science Letters, 220(1-2): 57-67.

Wang, X.-D., Sugiyama, T., 2000. Diversity and extinction patterns of Permian coral faunas of China. Lethaia, 33(4): 285-294.

Wang, Y., Jin, Y.G., 2000. Permian palaeogeographic evolution of the Jiangnan Basin, South China. Palaeogeography, Palaeoclimatology, Palaeoecology, 160(1-2): 35-44.

Wang, Y. et al., 2011. Progress, Problems and Prospects on the Stratigraphy and Correlation of the Kungurian Stage, Early Permian (Cisuralian) Series. Acta Geologica Sinica, 85(2): 387-398.

Wang, Z., 1994. Early Permian Conodonts from the Nashui Section, Luodian of Guizhou. Palaeoworld, 4: 203-224.

Wang, Z.H., 1978. Permian-Lower Triassic conodonts of the Liangshan area, southern Shanxi. Acta Palaeontologica Sinica, 17(2): 213-227.

Wardlaw, B.R., 2000. Guadalupian conodont biostratigraphy of the Glass and Del Norte Mountains. In:

Wardlaw, B.R., Grant, R.E., Rohr, D.M. (Eds.), The Guadalupian symposium-Smithsonian Contributions to the Earth Sciences, pp. 37-87.

Wardlaw, B.R., Gallegos, D.M., Chernykh, V.V., Snyder, W.S., 2015. Early Permian conodont fauna and stratigraphy of the Garden Valley Formation, Eureka County, Nevada. Micropaleontology, 61(4-5): 369-387.

Wardlaw, B.R., Grant, R.E., 1990. Conodont biostratigraphy of the Permian Road Canyon Formation, Glass Mountains, Texas. U.S. Geological Survey Bulletin, 1895: 63-66.

Wardlaw, B.R., Nestell, M.K., 2010. Latest Middle Permian conodonts from the Apache Mountains, West Texas. Micropaleontology, 56(1-2): 149-183.

Weidlich, O., 2002. Permian reefs re-examined: extrinsic control mechanisms of gradual and abrupt changes during 40 my of reef evolution. Geobios, 35, Supplement 1: 287-294.

Wignall, P.B. et al., 2009a. Volcanism, Mass Extinction, and Carbon Isotope Fluctuations in the Middle Permian of China. Science, 324: 1179-1182.

Wignall, P.B. et al., 2009b. Facies analysis and sea-level change at the Guadalupian–Lopingian Global Stratotype (Laibin, South China), and its bearing on the end-Guadalupian mass extinction. Journal of the Geological Society, 166(4): 655-666.

Youngquist, W.L., Hawley, R.W., Miller, A.K., 1951. Phosphoria conodonts from southeastern Idaho. Journal of Paleontology, 25(3): 356-364.

Zhang, K.X., Lai, X.L., Ding, M.H., Liu, J., 1995. Conodont Sequence and its Global Correlation of Permian-Triassic Boundary in Meishan Section, Changxing, Zhejiang Province. Earth Science-Journal of China University of Geosciences, 20(6): 669-676.

Zhang, Z., Wang, Y., Zheng, Q.F., 2015. Middle Permian smaller foraminifers from the Maokou Formation at the Tieqiao section, Guangxi, South China. Palaeoworld, 24(3): 263-276.

Figure captions

FIG. 1 Middle Permian palaeogeographic reconstructions of South China and Laibin area (after Wang and Jin, 2000; Shen et al., 2007).

FIG. 2 Field photographs of the studied section. A, an overview of the Chihsia Fm. in the lower part of the section. A digger in the far side (blue square) as scale. B, a close review of fine laminated Bed 111-112 transition (Roadian-Wordian boundary interval). The pen (~15 cm long) as scale.

FIG. 3 Log of the lower part of Tieqiao section (Asselian to Kungurian) with conodont ranges and zonation.

FIG. 4 Log of the middle part of Tieqiao section (Kungurian to Wordian) with conodont ranges and zonation. Keys are the same as in Fig. 3. Note that the reported occurrence of *Mesogondolella bisselli* in Bed 91 (Sha *et al.* 1990) cannot be confirmed by our dataset (for details see discussion of the *Sw. adjunctus* zone). Keys are the same as in figure 3.

FIG. 5 Log of the upper part of Tieqiao section (Wordian to Wuchiapingian) with conodont ranges and zonation. Keys are the same as in figure 3.

FIG. 6 Correlation chart of the Early-Middle Permian with standard conodont zonation (Henderson et al. 2012), Tieqiao (this study) and Nashui (Mei et al. 2002) sections. 1., *Pseudosweetognathus monocornus*; 2., *Hindeodus gulloides*; 3., *Gullodus sicilianus*; 4., *Hindeodus excavates*.

PLATE 1. SEM images of Tieqiao conodonts-genus *Sweetognathus*. Bar scale for 100 μm, 'a' for oral view, 'b' for lateral view. Default is oral view. **1, 7, 14, 17.** *Sweetognathus asymmetrica* **n. sp.,** 1, holotype, S1_018 (18-1); 7, paratype,

S1_037 (22-2); 14, S_001 (18-1); 17, S_006 (24A); **2, 16.** *Sweetognathus whitei* (Rhodes, 1963), 2, S1_019 (18-1); 16, S_005 (23A), this specimen shows a transition from *Sw. whitei* to *Sw. guizhouensis*; **3, 8.** *Pseudosweetognathus costatus* Wang, Ritter and Clark, 1987, 3, S1_021 (19-2), 8, S1_025 (21-2). **4.** *Sweetognathus* **sp.**, S1_023 (19-2); **5. Transitional form** from *Sw. inornatus* to *Sw. asymmetrica* **n. sp**., S1_038 (22-2); **6**. *Sweetognathus* **sp.,** S1_031 (22-1). **9.** *Sweetognathus* **sp. A.**, S1_026 (21-2); **10.** *Sweetognathus inornatus* Ritter, 1986, S1_030 (22-1); **11.** *Sweetognathus* **cf.** *bogoslovskajae* Kozur in Kozur and Mostler, 1976, S1_020 (18-1); **12, 15.** *Sweetognathus toriyamai* (Igo, 1981), 12, S_002 (17c), 15, juvenile form, S_003 (17c); **13.** *Sweetognathus clarki* (Kozur, 1976), S_004 (17c).

PLATE 2. SEM images of Tieqiao conodonts—genera *Sweetognathus, Pseudosweetognathus, Neostreptognathodus and Hindeodus.* Scale bar is for 100 µm, 'a' for oral view, 'b' for lateral view. Default is oral view. **1, 2, 4, 9.** *Sweetognathus bogoslovskajae* Kozur in Kozur and Mostler, 1976, 1, S1_039 (22-2), 2, S1_043 (24-3), 4, juvenile, S1_057 (39-1), 9, S1_051 (27-1); **3, 12.** *Sweetognathus guizhouensis* Bando et al., 1980, 3. S1_048 (26-3), 12. S1_055 (39-1); **5-7.** *Pseudosweetognathus costatus* Wang, Ritter and Clark, 1987, 5, S1_047 (26-2), 6. S1_049 (26-4), 7. S1_045 (25-2); **8.** *Neostreptognathodus prayi* Behnken, 1975, gerontic form, note the completely different platform shoulders compared to *Ps. costatus*, S1_046 (25-2); **10.** *Sweetognathus clarki*

Morphotype I, (Kozur, 1976), S1_050 (27-1); **11. *Sweetognathus inornatus*** Ritter, 1986, S1_053 (29-1); **13. *Hindeodus* aff. *catalanoi***, S1_022 (19-2); **14, 16, 17. *Hindeodus minutus*** (Ellison, 1941), 14, S1_044 (25-1), 16, S1_056 (39-1), 17, S1_052 (28-1); **15. *Hindeodus* sp.** S1_042 (23-3).

PLATE 3. SEM images of Tieqiao conodonts—genera *Sweetognathus* and *Pseudosweetognathus*. Scale bar is for 100 μm, 'a' for oral view, 'b' for lateral view. Default is oral view. **1-3. *Pseudosweetognathus costatus*** Wang, Ritter and Clark, 1987, 1. S1_065 (52-2); 2. S1_066 (58-1), 3. S1_068 (65-2); **4, 5. *Sweetognathus iranicus*** Kozur, 1975, 4, S1_069 (66-3), 5, S1_071 (71-1); **6. *Pseudosweetognathus monocornus*** (Dai and Zhang, 1989), S2_001 (94-2); **7, 9, 19. *Sweetognathus* sp.** 7. S1_072 (90-7), 9. S2_002 (97-2), 19. S2_020 (100-1); **8, 10, 11. *Sweetognathus adjunctus*** (Behnken, 1975), 8. S2_004 (97-2), 10. S2_005 (97-2), 11. S1_076 (91-1); **12, *Sweetognathus* cf. *paraguizhouensis*** S1_078 (91-3); **13. Transitional form** between *Sweetognathus iranicus* and *Sweetognathus hanzhongensis*, S2_007 (99-4); **14. *Sweetognathus subsymmetrics*** Wang, Ritter and Clark, 1987, S2_039 (100-3); **15-18. *Sweetognathus hanzhongensis*** (Wang, 1978), 15, S2_038 (100-5), 16, S2_018 (100-1), 17, S2_010 (100-1), 18, S2_028 (100-3).

PLATE 4. SEM images of Tieqiao conodonts—genera *Sweetognathus*, *Gullodus*,

Hindeodus and *Pseudohindeodus*. Scale bar is for 100 μm, 'a' for oral view, 'b' for lateral view. Default is oral view. **1.** *Sweetognathus* **sp.** S2_049 (102-2); **2-4.** *Sweetognathus subsymmetrics* Wang, Ritter and Clark, 1987, 2. S2_051 (102-3); 3. S2_056 (102-4); 4. S2_058 (102-4); **5, 15.** *Sweetognathus iranicus* Kozur, 1975, 5, S2_082 (105-3), 15, S2_072 (103-2); **6-7.** *Gullodus tieqiaoensis* **n. sp.**, 6. holotype, S1_060 (41-1), 7. paratype, S1_062 (41-2); **8.** *Gullodus sicilianus* (Bender and Stoppel, 1956), S3_020 (115-4); **9, 10, 16, 18. Transitional forms between** *Hindeodus* **and** *Pseudohindeodus.* Note that these elements developed weak apron structures on basal cavities. 9. S1_074 (91-1), 10. S1_075 (91-1), 16. S2_057 (102-4), 18. S2_053 (102-3); **11, 12.** *Gullodus duani* Mei et al., 2002, 11. S1_013 (TQ-28), 12. S3_022 (115-7); **13.** *Pseudohindeodus elliptica* **n. sp.** Sun and Lai, paratype, S2_075 (104-2); **14.** *Pseudohindeodus ramovsi* Gullo and Kozur, 1992, S2_073 (103-4); **17.** *Hindeodus* **cf.** *wordensis* Wardlaw, 2000; 17, S2_060 (102-5); **19, 20.** *Hindeodus* **cf.** *julfensis* 19, S2_014 (100-1), 20. S2_011 (100-1); **21.** *Hindeodus* **cf.** *permicus,* S2_050 (102-2); **22, 36.** *Hindeodus* **sp.** 22, S2_061 (102-5), 36, S2_022 (100-3); **23, 26.** *Hindeodus* **sp. A**. 23, S2_068 (103-2); 26, S2_084 (106-1). **24, 25, 27, 30-32, 34, 35.** *Hindeodus permicus* (Igo, 1981) 24. S2_081 (105-3), 25. S2_034 (100-4), 27. S2_026 (100-3), 30. S2_083 (105-3), 31. S2_016 (100-1), 32. S2_062 (103-1), 34. S2_071 (103-2); 35, S2_067 (103-2). **28, 29.** *Hindeodus minutus* (Ellison, 1941), 28. S2_027 (100-3); 29. S2_021 (100-2); **33.** *Hindeodus golloides* Kozur and Mostler, 1995, S2_066 (103-2).
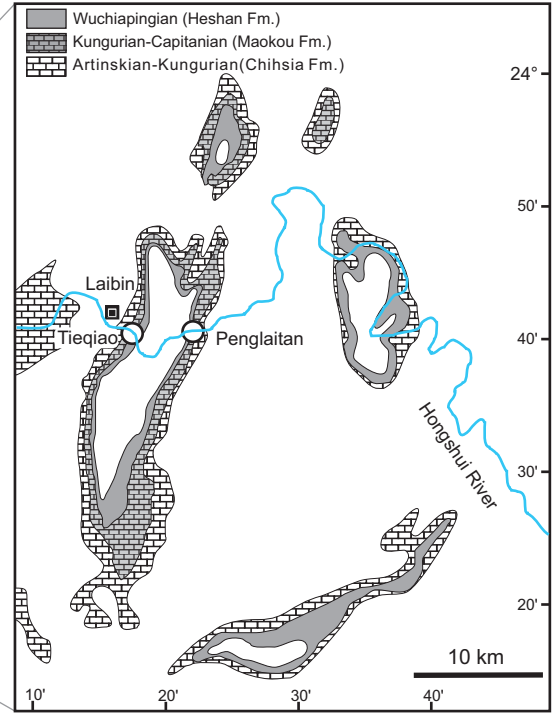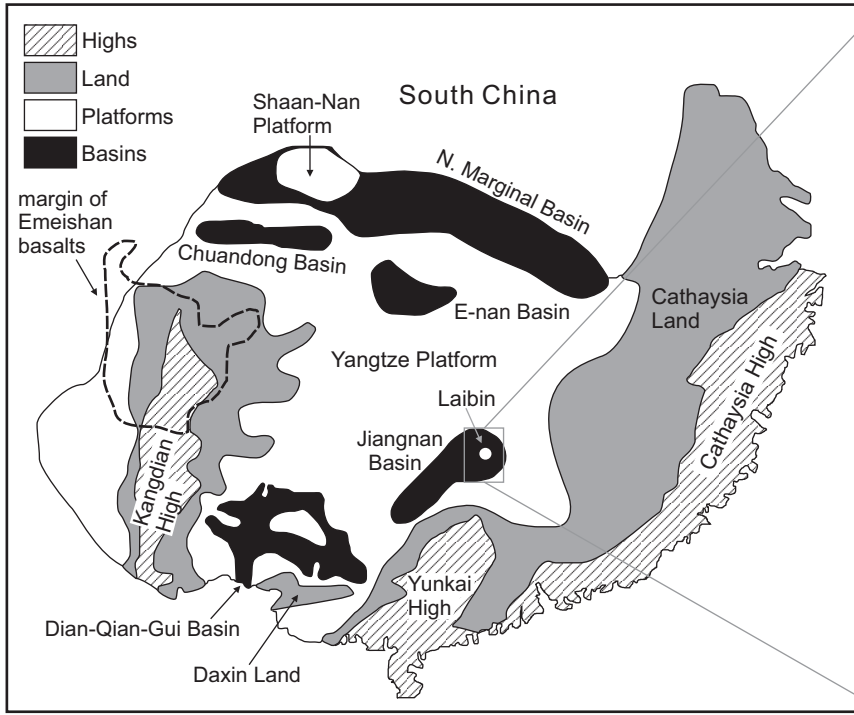
PLATE 5. SEM images of Tieqiao conodonts—genera *Mesogondolella* and *Jinogondolella*. Scale bar is for 100 μm, 'a' for oral view, 'b' for lateral view. Default is oral view. **1, 7. transitional type between *M. lamberti* to *J. nankingensis*,** 1, S3_001 (109-2), 7, S3_012 (113-2); **2, 5, 9. *Jinogondolella nankingensis*** (Ching, 1960), 2. S3_002 (109-2); 5. S3_007 (111-1); 9. S3_011 (111-5); **3, 8. *Mesogondolella* sp.**, 3. S3_004 (109-3), 8. S3_013 (113-7); **4. *Mesogondolella* cf. *idahoensis*** (Youngquist, Hawley, Miller, 1951), S3_005 (110-2); **6. *Mesogondolella sicilliensis*** (Kozur, 1975), S3_006 (111-1); **10-11. *Jinogodolella errata*** Wardlaw and Nestell, 2000, 10. S3_019 (115-3), 11. S3_017 (115-2); **12. *Jinogondolella aserrata*** (Clark and Behnken, 1979), S3_021 (115-4); **13, 16. *Jinogondolella* sp.,** 13. SP_051 (115-3), 16, S3_037 (116-7); **14, 15. *Jinogondolella postserrata*** (Behnken, 1975), S3_028 (116-1); 15. S3_036 (116-7); **17, 18. *Jinogondolella shannoni*** (Wardlaw, 1994), 17. S3_040 (116-8); 18, S3_030 (116-2); **19. *Jinogondolella altudaensis*** (Kozur, 1992), S3_033 (116-3).

PLATE 6. SEM images of Tieqiao conodonts—genera *Jinogondolella* and *Clarkina*. Scale bar is for 100 μm, 'a' for oral view, 'b' for lateral view and 'c' for back view. Default is oral view. **1. *Jinogondolella prexuanhanensis*** (Mei and Wardlaw, 1994), S4_004 (TQ-11); **2. *Jinogondolella* cf. *prexuanhanensis*** SP_010 (118-2);

3-5. *Jinogondolella shannoni* (Wardlaw, 1994), 3. S3_062 (118-2); 4. S4_006 (TQ-17+); 5, SP_014 (118-2); **6, 17. *Jinogondolella* sp.,** 6, SP_013 (118-2), 17, S_035 (119A); **7. *Jinogondolella xuanhanensis*** (Mei and Wardlaw, 1994), 06-70_023 (TQ-6f); **8-11. *Jinogondolella granti*** (Mei and Wardlaw, 1994), 8. 06-70_024 (TQ-6f), 9. 06-70_022 (TQ-6f), 10. TQ6f_010 (TQ-6f), 11. 06-70_027b (TQ-6f); **12-13. *Clarkina postbitteri*** Mei and Warldlaw, 1994, 12. S6_054 (TQ-1), 13. C6_040a (TQ-1). **14. *Clarkina* sp.,** S6_055 (TQ-1); **15. *Clarkina transcaucasica*** Gullo and Kozur, 1992, S4_003 (134-9); **16. *Clarkina hongshuiensis*** Henderson, Mei and Wardlaw, 2002, S_029 (TQ-1).

PLATE 7. SEM images of Tieqiao conodonts—genera *Hindeodus, Jinogondolella, Mesogondolella, Pseudohindeodus* and *Sweetognathus*. Scale bar is for 100 μm, 'a' for oral view, 'b' for lateral view. Default is oral view. **1, transitional form between *Sweetognathus bogoslovskajae* and *Sweetognathus inornatus*,** S_007 (24A); **2. *Sweetognathus inornatus*** Ritter, 1986, S_008 (26C); **3. *Sweetognathus fengshanensis*** Mei and Wardlaw, 1998, S_016 (117-3); **4. *Mesogondolella idahoensis*** (Youngquist, Hawley and Miller, 1951), S_009 (109-2); **5. *Jinogondolella palmata*** (Nestell and Wardlaw, 2010), S_025 (111-1-2); **6-8. *Hindeodus catalanoi*** (Gullo and Kozur, 1992), 6, S3_052 (117-2), 7, S3_052 (117-2), 8, S3_043 (116-12); **9-10. *Sweetognathus hanzhongensis*** (Wang, 1978), 9, S4_012 (TQ-25), 10, S_025 (115-8). **11-12. *Pseudohindeodus augustus*** (Igo, 1981), 11, S7_007 (102-4), 12, S7_005 (102-4). **13.**

***Pseudohindeodus* sp.** S7_003 (104-2). **14. *Pseudohindeodus elliptica* n. sp.** Sun

and Lai, holotype, S7_001 (104-2).

Left map:

Highs
Land
Platforms
Basins

margin of
Emeishan
basalts

South China

Shaan-Nan
Platform

N. Marginal Basin

Chuandong Basin

E-nan Basin

Cathaysia
Land

Yangtze Platform

Laibin

Cathaysia High

Jiangnan
Basin

Kangdian High

Dian-Qian-Gui Basin

Daxin Land

Yunkai
High

Right map:

Wuchiapingian (Heshan Fm.)
Kungurian-Capitanian (Maokou Fm.)
Artinskian-Kungurian (Chihsia Fm.)

24°

50'

Laibin

40'

Tieqiao

Penglaitan

Hongshui River

30'

20'

10 km

10'   20'   30'   40'

Conodont Zonation

Stage | Frm. | Unit | Bed | Thick.

Wuchiap | Heshan | XI | 120
X | 119
118
117
116
115
114
113

Capitanian | Maokou Formation | IX

Wordian | VIII | VII

M W P G

Sample position

Pseduosw. monocornus

Pseudohind. ramovsi

Sweetognathus fenshanensis

Sw. hanzhongensis

Gullodus sicillanus

Gullodus duani

Hindeodus catalanoi

H. excavatus

J. aserrata

J. errata

J.postserrata

J. shannoni

J. altudaensis

J. prexuanhanensis

J. xuanhanensis

J. granti

C.hongshuiensis

C.postbitteri

Main | Subordinate

C. postbitteri

C.hongshuiensis

J. granti

J. xuanhanensis

J. prexuanhanensis

J. altudaensis

J. shannoni

J.postserrata

J. aserrata

H. excavatus

Gullodus duani

G. sicillanus

Pseudohindeodus ramovsi

Sweetognathus, Pseduosw.

Hindeodus, Gullodus

Jinogondolella & Clarkina

1a 1b 2a 2b 2c 3a 3b 4a 4b

5a 5b 5c 6a 6b 7a 7b 8a 8b

9a 9b 10a 10b 11a 11b 12a 12b 13a 13b

14a 14b 15a 15b 16a 16b 17a 17b